Stiffness modeling of 3RRR Parallel Spherical Manipulator

Dmitry Popov
Innopolis University
Innopolis, Russia
d.popov@innopolis.ru

Valeria Skvortsova
Innopolis University
Innopolis, Russia
v.skvortsova@innopolis.ru

Alexandr Klimchik
Innopolis University
Innopolis, Russia
a.klimchik@innopolis.ru

Abstract

The paper deals with stiffness modeling of 3RRR parallel spherical manipulator. This manipulator is proposed to be used as a rehabilitation device for wrist trauma. The desired elastostatic model is obtained using a matrix structural analysis approach (MSA) which divides robot representation into two sets of constraints describing elasticity of the links and connection between them. The model operates with matrices of size 84x84 for each leg. As a result, the closed-form solution for the Cartesian stiffness matrix for this type of robot is derived.

1 Introduction

In the last few decades, various types of robots were used for joint rehabilitation with both, serial and parallel structure. Examples of this rehabilitation devices are: The Wrist Gimbal [1] is a serial three degree-of-freedom (DOF) exoskeleton developed for forearm and wrist rehabilitation, compared to other devices the Wrist Gimbal has a large desirable workspace; A Haptic Knob [2] is 2 DOF robotic interface to train opening/closing of the hand and knob manipulation, its mechanical design based on two parallelogram structures holding an exchangeable button, with possibility to adapt the interface to various hand sizes and finger orientations; MAHI Exo II [3] is a 5 DOF robotic exoskeleton for rehabilitation of upper extremity after stroke, spinal cord injury, or other brain injuries, this exoskeleton is comprised of a revolute joint at the elbow, a revolute joint for forearm rotation, and a 3-RPS (revolute-prismatic-spherical) serial-in-parallel wrist.

In this work, the spherical parallel robot is proposed for this task. The use of this kind of robot is justified since it corresponds to a common spherical 3-degree-of-freedom motion in biological systems like in shoulder, hip and wrist joints. In parallel manipulators all actuators are usually fixed to the base of the manipulator, there providing better load-carrying capacity and better dynamic properties. These advantages of parallel spherical manipulator lead to far less intuitive kinematic, dynamic and elastostatic calculations than in a common serial manipulator.

For the stiffness modeling three main approaches are distinguished in literature: the finite elements analysis (FEA) [4], the matrix structural analysis (MSA) [5, 6, 7] and the virtual joint method (VJM) [8, 9, 10]. In FEA method, a physical model of the robot is decomposed into a number of small elements

with compliant relation between these elements [11]. This method offers highly accurate solutions, but require large number of finite elements, which greatly increases computational complexity. The MSA uses the main ideas of the FEA but at the same time handles large complaint elements (as robot links), which reduces computational efforts [5]. The last method is the VJM that is based on the expansion of the traditional geometrical rigid-body model of the robot with virtual joints corresponding to the compliances of the links and joints [8]. In this work MSA technique is used.

2 Robot Description

A spherical 3-DOF parallel manipulator with revolute actuators for wrist rehabilitation consists of 3 serial kinematic chains and an end-effector platform [12]. The prototype of this robot is shown in fig. 1a. Each chain has 2 curved links and 3 revolute joints, joint on the base of the robot is actuated with a motor. The kinematic representation of this robot is presented in fig. 1b, and can be described with a two pyramid. The structure of the manipulator is such that the axes of all 9 revolute joints intersect at one common point O, which will henceforth be called the center of the mechanism. All the moving bodies are in pure rotation with respect to this point.

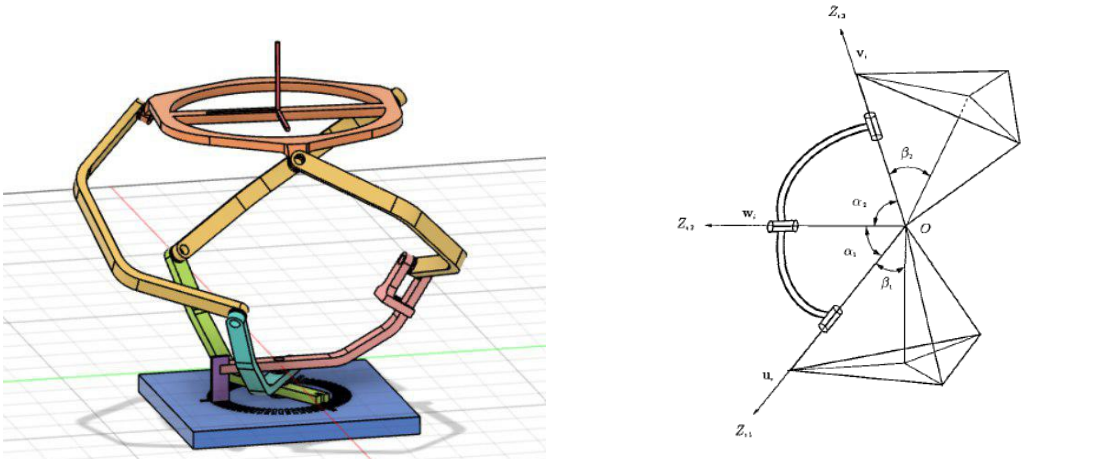

(a) Robot prototype in CAD

(b) Kinematics description of parallel spherical manipulator for i-th leg

Figure 1: Kinematic model of a parallel spherical manipulator

Table 1: DH parameters of the robot

Frame	α_n	θ_n
Base platform (BP)	$\beta_1 + \pi$	$-\eta_i$
Link 1 (L1)	α_1	θ_i
Link 2 (L2)	α_2	μ_{1_i}
End-effector platform (EEP)	0	μ_{2_i}

The kinematic structure of the robot leg could be described using DH notation (Table 1). Where α_1 and α_2 are the first and the second bend angle of links, θ_i is an active joint rotation angle, μ_{1i} is the first passive joint rotation angle, μ_{2i} is the second passive joint rotation angle and $\eta_i = \frac{2(i-1)\pi}{N}$ where N is a number of legs, $i = 1, 2...N$ is an angle of leg connection on the lower platform.

3 Stiffness Analysis

As a complex parallel structure, the use of the MSA technique is reasonable for the spherical parallel manipulator stiffness modeling. The fundamentals of these technique in general form and all theoretical

basis could be found in [13]. Here we present only the final closed-form solution for this type of robot. The stiffness modeling itself would be later used for design optimization in a similar way as in [14].

3.1 Link Stiffness

Firstly, stiffness matrices of links in the global frame should be obtained. In general case, the stiffness matrix of the link is obtained from the FEA modeling in CAD software or approximated with cantilever beam for which there is a known closed-form equation. Unlike most robotic manipulators, spherical wrist robot legs consist of only curved beams, so different approximation is required. For this purpose stiffness of each link is calculated by the Euler-Bernoulli stiffness model of a cantilever.

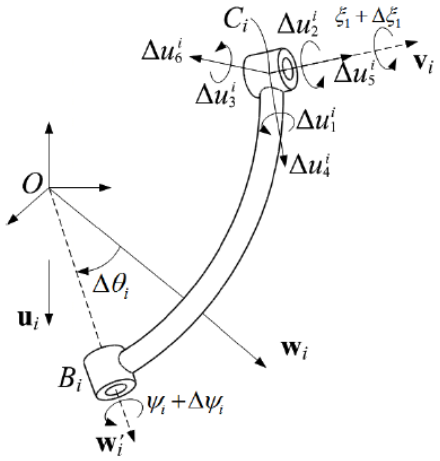

Figure 2: Upper link deflections and joint variations in the i-th leg.

In Fig. 2, Δu_1, Δu_2 and Δu_3 show torque vector while Δu_4, Δu_5 and Δu_6 show the force vector directions, thus using Castigliano's theorem, the compliance matrix of the curved link takes the form of:

$$K_\theta^{L\,-1} = \begin{bmatrix} C_{11} & C_{12} & 0 & 0 & 0 & C_{16} \\ C_{12} & C_{22} & 0 & 0 & 0 & C_{26} \\ 0 & 0 & C_{33} & C_{34} & C_{35} & 0 \\ 0 & 0 & C_{34} & C_{44} & C_{45} & 0 \\ 0 & 0 & C_{35} & C_{45} & C_{55} & 0 \\ C_{16} & C_{26} & 0 & 0 & 0 & C_{66} \end{bmatrix} \tag{1}$$

the elements of this matrix are:

$$C_{11} = \frac{R}{2}\left(\frac{s_1}{GI_x} + \frac{s_2}{EI_y}\right); \quad C_{12} = \frac{s_8 R}{2}\left(\frac{1}{GI_x} - \frac{1}{EI_y}\right); \quad C_{16} = \frac{R^2}{2}\left(\frac{s_2}{EI_y} - \frac{s_7}{EI_x}\right)$$
$$C_{22} = \frac{R}{2}\left(\frac{s_2}{GI_x} + \frac{s_1}{EI_y}\right); \quad C_{26} = \frac{R^2}{2}\left(\frac{s_4}{GI_x} - \frac{s_2}{EI_y}\right); \quad C_{33} = \frac{R\alpha_L}{EI_z}; \quad C_{34} = \frac{s_5 R^2}{EI_z}$$
$$C_{35} = \frac{s_6 R^2}{EI_z}; \quad C_{44} = \frac{R}{2A}\left(\frac{s_1}{E} + \frac{s_2}{G}\right) + \frac{s_3 R^3}{2EI_z}; \quad C_{45} = \frac{s_8 R}{2A}\left(\frac{1}{E} - \frac{1}{G}\right) + \frac{s_4 R^3}{2EI_z}$$
$$C_{55} = \frac{R}{2A}\left(\frac{s_1}{E} + \frac{s_2}{G}\right) + \frac{s_2 R^3}{2EI_z}; \quad C_{66} = \frac{R\alpha_L}{GA} + \frac{R^3}{2}\left(\frac{s_3}{GI_x} + \frac{s_2}{EI_y}\right)$$

with:
$s_1 = \alpha_L + \sin\alpha_L \cos\alpha_L$
$s_2 = \alpha_L - \sin\alpha_L \cos\alpha_L$

$s_3 = 3\alpha_L + \sin\alpha_L \cos\alpha_L/2 - 4\sin\alpha_L$
$s_4 = 1 - \cos\alpha_L - sin^2\alpha_L/2$
$s_5 = \sin\alpha_L - \alpha_L$
$s_6 = \cos\alpha_L - 1$
$s_7 = 2\sin\alpha_L - \alpha_L - \sin\alpha_L \cos\alpha_L$
$s_8 = -\sin^2\alpha_L$

where E is Young's modulus and $G = E/2(1+\nu)$ is the shear modulus with the Poisson's ration ν. I_x, I_y and I_z are moments of inertia, respectively. A is the area of the cross-section.

3.2 Robot Stiffness

The first step in MSA modeling is deriving the MSA model of the robot. Here, two cases are possible. In the first method (fig.3), the robot is split into four parts: the robot platform and three legs. This allows taking into account a complex platform elasticity of the robot if needed. In the second case, robot split only into three leg, where each leg has part of the end-effector platform as the last link (fig. 3a). For simplicity, let's assume that end-effector platform is rigid, so we can easily implement second method.

Since the spherical wrist robot is symmetrical, the legs of the robot are the same, so equations only for one leg are presented. According to node numbering in fig. 3a, links 2-3 and 4-5 are flexible and their stiffness is described by equations presented earlier, link 6-e is rigid, joints 3-4 and 5-6 are passive and joint 1-2 is active and elastic.

The equations notation is the following: Δt_i and Δt_j are the deflections at the link ends,W_i and W_j are the link end wrenches, i and j are the node indices, and $K^{11}_{i,j}$, $K^{12}_{i,j}$, $K^{21}_{i,j}$, $K^{22}_{i,j}$ are 6x6 stiffness matrices.

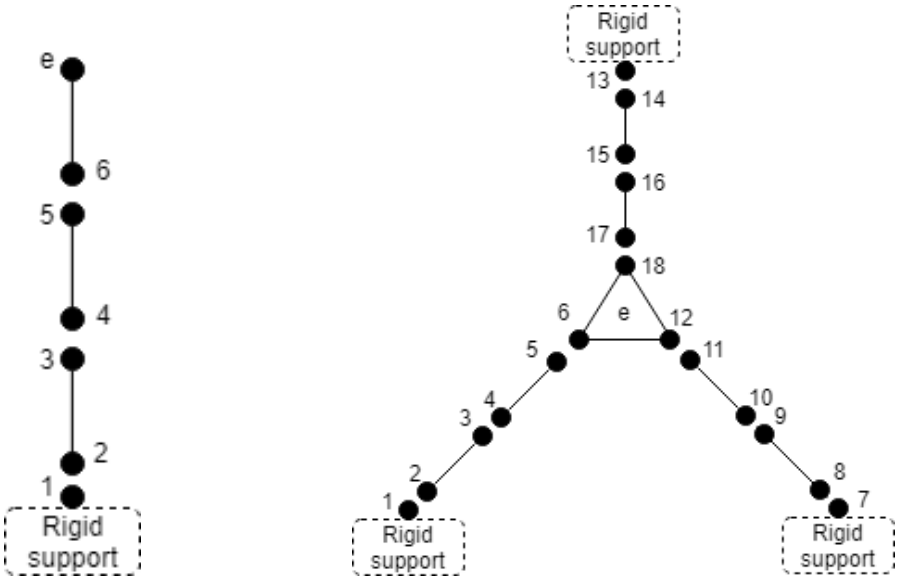

(a) The MSA model of i-th leg (b) The MSA model for full robot

Figure 3: MSA model of a parallel spherical manipulator

The node 1 is connected to the rigid base and described by the following constraint equation:

$$\begin{bmatrix} 0_{6\times6} & I_{6\times6} \end{bmatrix} \begin{bmatrix} W_1 \\ \Delta t_1 \end{bmatrix} = 0 \tag{2}$$

Flexible links 2-3 and 4-5 constraints on deflection and loading could be described as:

$$\begin{bmatrix} -I_{6\times6} & 0_{6\times6} & 0_{6\times6} & 0_{6\times6} & K^{11}_{2,3} & K^{12}_{2,3} & 0_{6\times6} & 0_{6\times6} \\ 0_{6\times6} & -I_{6\times6} & 0_{6\times6} & 0_{6\times6} & K^{12}_{2,3} & K^{22}_{2,3} & 0_{6\times6} & 0_{6\times6} \\ 0_{6\times6} & 0_{6\times6} & -I_{6\times6} & 0_{6\times6} & 0_{6\times6} & 0_{6\times6} & K^{11}_{4,5} & K^{12}_{4,5} \\ 0_{6\times6} & 0_{6\times6} & 0_{6\times6} & -I_{6\times6} & 0_{6\times6} & 0_{6\times6} & K^{12}_{4,5} & K^{22}_{4,5} \end{bmatrix} \begin{bmatrix} W_2 \\ W_3 \\ W_4 \\ W_5 \\ \Delta t_2 \\ \Delta t_3 \\ \Delta t_4 \\ \Delta t_5 \end{bmatrix} = \begin{bmatrix} 0 \\ 0 \\ 0 \\ 0 \end{bmatrix} \tag{3}$$

Rigid platform presented as a rigid link 6-e:

$$\begin{bmatrix} 0_{6\times6} & 0_{6\times6} & D_{6,e} & -I_{6\times6} \\ I_{6\times6} & D^T_{6,e} & 0_{6\times6} & 0_{6\times6} \end{bmatrix} \begin{bmatrix} W_6 \\ W_e \\ \Delta t_6 \\ \Delta t_e \end{bmatrix} = \begin{bmatrix} 0 \\ 0 \end{bmatrix} \tag{4}$$

where

$$D_{6,e} = \begin{bmatrix} I_{3\times3} & [d_{6,e}]^T_\times \\ 0_{3\times3} & I_{3\times3} \end{bmatrix}$$

$[d_{6,e}]_\times$ is denotes the 3×3 skew-symmetric matrix derived from the vector $d_{6,e}$ describes the link geometry and is directed from the 6th to the e-th node.

Active elastic joint 1-2 is described by the following equation:

$$\begin{bmatrix} 0_{5\times6} & 0_{5\times6} & \lambda^r_{1,2} & -\lambda^r_{1,2} \\ I_{6\times6} & I_{6\times6} & 0_{6\times6} & 0_{6\times6} \\ \lambda^e_{1,2} & 0_{1\times6} & K_{act}\lambda^e_{1,2} & -K_{act}\lambda^e_{1,2} \end{bmatrix} \begin{bmatrix} W_1 \\ W_2 \\ \Delta t_1 \\ \Delta t_2 \end{bmatrix} = \begin{bmatrix} 0 \\ 0 \\ 0 \end{bmatrix} \tag{5}$$

where K_{act} is a stiffness of the actuator.

The passive joints 3-4 and 5-6:

$$\begin{bmatrix} 0_{5\times6} & 0_{5\times6} & 0_{5\times6} & 0_{5\times6} & \lambda^r_{3,4} & -\lambda^r_{3,4} & 0_{5\times6} & 0_{5\times6} \\ \lambda^r_{3,4} & \lambda^r_{3,4} & 0_{5\times6} & 0_{5\times6} & 0_{5\times6} & 0_{5\times6} & 0_{5\times6} & 0_{5\times6} \\ \lambda^p_{3,4} & 0_{1\times6} & 0_{1\times6} & 0_{1\times6} & 0_{1\times6} & 0_{1\times6} & 0_{1\times6} & 0_{1\times6} \\ 0_{1\times6} & \lambda^p_{3,4} & 0_{1\times6} & 0_{1\times6} & 0_{1\times6} & 0_{1\times6} & 0_{1\times6} & 0_{1\times6} \\ 0_{5\times6} & 0_{5\times6} & 0_{5\times6} & 0_{5\times6} & 0_{5\times6} & 0_{5\times6} & \lambda^r_{5,6} & -\lambda^r_{5,6} \\ 0_{1\times6} & 0_{1\times6} & \lambda^r_{5,6} & \lambda^r_{5,6} & 0_{5\times6} & 0_{5\times6} & 0_{5\times6} & 0_{5\times6} \\ 0_{5\times6} & 0_{5\times6} & \lambda^p_{5,6} & 0_{1\times6} & 0_{1\times6} & 0_{1\times6} & 0_{1\times6} & 0_{1\times6} \\ 0_{1\times6} & 0_{1\times6} & 0_{1\times6} & \lambda^p_{5,6} & 0_{1\times6} & 0_{1\times6} & 0_{1\times6} & 0_{1\times6} \end{bmatrix} \begin{bmatrix} W_3 \\ W_4 \\ W_5 \\ W_6 \\ \Delta t_3 \\ \Delta t_4 \\ \Delta t_5 \\ \Delta t_6 \end{bmatrix} = \begin{bmatrix} 0 \\ 0 \\ 0 \\ 0 \\ 0 \\ 0 \end{bmatrix} \tag{6}$$

where

$$\lambda^r = \begin{bmatrix} 1 & 0 & 0 & 0 & 0 & 0 \\ 0 & 1 & 0 & 0 & 0 & 0 \\ 0 & 0 & 1 & 0 & 0 & 0 \\ 0 & 0 & 0 & R_{11} & R_{12} & R_{13} \\ 0 & 0 & 0 & R_{21} & R_{22} & R_{23} \end{bmatrix}; \quad \lambda^e = \begin{bmatrix} 0 & 0 & 0 & R_{31} & R_{32} & R_{33} \end{bmatrix}$$

R_{ij} is ijth element of rotation matrix in joint. λ^p calculated the same way as λ^e

The external loading denotes by the following equation:

$$\begin{bmatrix} I_{6\times6} & 0_{6\times6} \end{bmatrix} \begin{bmatrix} W_e \\ \Delta t_e \end{bmatrix} = W_{ext} \tag{7}$$

Now we can aggregate the equations (2), (3), (4), (5), (6) and (7) to the following type:

$$\begin{bmatrix} A & B \\ C & D \end{bmatrix} \begin{bmatrix} W_{ag} \\ \Delta t_{ag} \\ \Delta t_e \end{bmatrix} = \begin{bmatrix} 0 \\ W_{ext} \end{bmatrix} \tag{8}$$

where

$$B = \begin{bmatrix} 0_{30\times 6} \\ -I_{6\times 6} \\ 0_{42\times 6} \end{bmatrix}; \quad C = \begin{bmatrix} 0_{6\times 36} & I_{6\times 6} & 0_{6\times 36} \end{bmatrix}; \quad D = 0_{6\times 6}$$

$$A = \begin{bmatrix}
0_{6\times6} & 0_{6\times6} & 0_{6\times6} & 0_{6\times6} & 0_{6\times6} & 0_{6\times6} & 0_{6\times6} & I_{6\times6} & 0_{6\times6} & 0_{6\times6} & 0_{6\times6} & 0_{6\times6} & 0_{6\times6} \\
0_{6\times6} & -I_{6\times6} & 0_{6\times6} & 0_{6\times6} & 0_{6\times6} & 0_{6\times6} & 0_{6\times6} & 0_{6\times6} & K^{11}_{2,3} & K^{12}_{2,3} & 0_{6\times6} & 0_{6\times6} & 0_{6\times6} \\
0_{6\times6} & 0_{6\times6} & -I_{6\times6} & 0_{6\times6} & 0_{6\times6} & 0_{6\times6} & 0_{6\times6} & 0_{6\times6} & K^{12}_{2,3} & K^{22}_{2,3} & 0_{6\times6} & 0_{6\times6} & 0_{6\times6} \\
0_{6\times6} & 0_{6\times6} & 0_{6\times6} & -I_{6\times6} & 0_{6\times6} & 0_{6\times6} & 0_{6\times6} & 0_{6\times6} & 0_{6\times6} & 0_{6\times6} & K^{11}_{4,5} & K^{12}_{4,5} & 0_{6\times6} \\
0_{6\times6} & 0_{6\times6} & 0_{6\times6} & 0_{6\times6} & -I_{6\times6} & 0_{6\times6} & 0_{6\times6} & 0_{6\times6} & 0_{6\times6} & 0_{6\times6} & K^{12}_{4,5} & K^{22}_{4,5} & 0_{6\times6} \\
0_{6\times6} & 0_{6\times6} & 0_{6\times6} & 0_{6\times6} & 0_{6\times6} & 0_{6\times6} & 0_{6\times6} & 0_{6\times6} & 0_{6\times6} & 0_{6\times6} & 0_{6\times6} & 0_{6\times6} & D_{6,e} \\
0_{6\times6} & 0_{6\times6} & 0_{6\times6} & 0_{6\times6} & 0_{6\times6} & I_{6\times6} & D^T_{6,e} & 0_{6\times6} & 0_{6\times6} & 0_{6\times6} & 0_{6\times6} & 0_{6\times6} & 0_{6\times6} \\
0_{5\times6} & 0_{5\times6} & 0_{5\times6} & 0_{5\times6} & 0_{5\times6} & 0_{5\times6} & 0_{5\times6} & \lambda^r_{1,2} & -\lambda^r_{1,2} & 0_{5\times6} & 0_{5\times6} & 0_{5\times6} & 0_{5\times6} \\
I_{6\times6} & I_{6\times6} & 0_{6\times6} & 0_{6\times6} & 0_{6\times6} & 0_{6\times6} & 0_{6\times6} & 0_{6\times6} & 0_{6\times6} & 0_{6\times6} & 0_{6\times6} & 0_{6\times6} & 0_{6\times6} \\
\lambda^e_{1,2} & 0_{1\times6} & 0_{1\times6} & 0_{1\times6} & 0_{1\times6} & 0_{1\times6} & 0_{1\times6} & K_a\lambda^e_{1,2} & -K_a\lambda^e_{1,2} & 0_{1\times6} & 0_{1\times6} & 0_{1\times6} & 0_{1\times6} \\
0_{5\times6} & 0_{5\times6} & 0_{5\times6} & 0_{5\times6} & 0_{5\times6} & 0_{5\times6} & 0_{5\times6} & 0_{5\times6} & 0_{5\times6} & \lambda^r_{3,4} & -\lambda^r_{3,4} & 0_{5\times6} & 0_{5\times6} \\
0_{5\times6} & 0_{5\times6} & \lambda^r_{3,4} & \lambda^r_{3,4} & 0_{5\times6} & 0_{5\times6} & 0_{5\times6} & 0_{5\times6} & 0_{5\times6} & 0_{5\times6} & 0_{5\times6} & 0_{5\times6} & 0_{5\times6} \\
0_{1\times6} & 0_{1\times6} & \lambda^p_{3,4} & 0_{1\times6} & 0_{1\times6} & 0_{1\times6} & 0_{1\times6} & 0_{1\times6} & 0_{1\times6} & 0_{1\times6} & 0_{1\times6} & 0_{1\times6} & 0_{1\times6} \\
0_{1\times6} & 0_{1\times6} & 0_{1\times6} & \lambda^p_{3,4} & 0_{1\times6} & 0_{1\times6} & 0_{1\times6} & 0_{1\times6} & 0_{1\times6} & 0_{1\times6} & 0_{1\times6} & 0_{1\times6} & 0_{1\times6} \\
0_{5\times6} & 0_{5\times6} & 0_{5\times6} & 0_{5\times6} & 0_{5\times6} & 0_{5\times6} & 0_{5\times6} & 0_{5\times6} & 0_{5\times6} & 0_{5\times6} & 0_{5\times6} & \lambda^r_{5,6} & -\lambda^r_{5,6} \\
0_{5\times6} & 0_{5\times6} & 0_{5\times6} & 0_{5\times6} & \lambda^r_{5,6} & \lambda^r_{5,6} & 0_{5\times6} & 0_{5\times6} & 0_{5\times6} & 0_{5\times6} & 0_{5\times6} & 0_{5\times6} & 0_{5\times6} \\
0_{1\times6} & 0_{1\times6} & 0_{1\times6} & 0_{1\times6} & \lambda^p_{5,6} & 0_{1\times6} & 0_{1\times6} & 0_{1\times6} & 0_{1\times6} & 0_{1\times6} & 0_{1\times6} & 0_{1\times6} & 0_{1\times6} \\
0_{1\times6} & 0_{1\times6} & 0_{1\times6} & 0_{1\times6} & 0_{1\times6} & \lambda^p_{5,6} & 0_{1\times6} & 0_{1\times6} & 0_{1\times6} & 0_{1\times6} & 0_{1\times6} & 0_{1\times6} & 0_{1\times6}
\end{bmatrix}$$

So, the Cartesian stiffness matrix K_{Ci} is found according to the following equation:

$$K_{Ci} = D - CA^{-1}B \tag{9}$$

Then the resulting stiffness matrix K_C of the whole manipulator could be found as:

$$K_C = \sum_{i=1}^{3} K_{Ci} \tag{10}$$

It should be noted, that rank of the K_{Ci} will not be full, because of the passive joints, but after assembly step, where stiffness matrices of all legs are combined K_C, rank of this matrix will be full.

4 Conclusions

In this work, closed-form equations for the Cartesian stiffness matrix of the spherical parallel manipulator are presented. The desired models were obtained using the enhanced matrix structural analysis (MSA) approach that is able to analyze the under-actuated and over-constrained structures with numerous passive joints. In order to obtain stiffness model, the robot was split into 3 legs, each of them supporting part of the end-effector platform. The total robot stiffness matrix was obtained in two steps: calculating stiffness for each leg and aggregating legs in total robot structure. The algorithm deals with matrices of size 84x84 for each leg and computationally light.

In future work, the stiffness model will be used for design optimization.

5 Acknowledgements

This work was supported by RFBR grant 18-38-20186

References

[1] J. A. Martinez, P. Ng, S. Lu, M. S. Campagna, and O. Celik, "Design of wrist gimbal: A forearm and wrist exoskeleton for stroke rehabilitation," in *2013 IEEE 13th International Conference on Rehabilitation Robotics (ICORR)*, pp. 1–6, IEEE, 2013.

[2] O. Lambercy, L. Dovat, R. Gassert, E. Burdet, C. L. Teo, and T. Milner, "A haptic knob for rehabilitation of hand function," *IEEE Transactions on Neural Systems and Rehabilitation Engineering*, vol. 15, no. 3, pp. 356–366, 2007.

[3] A. U. Pehlivan, O. Celik, and M. K. O'Malley, "Mechanical design of a distal arm exoskeleton for stroke and spinal cord injury rehabilitation," in *2011 IEEE International Conference on Rehabilitation Robotics*, pp. 1–5, IEEE, 2011.

[4] A. Taghaeipour, J. Angeles, and L. Lessard, "Online computation of the stiffness matrix in robotic structures using finite element analysis," *Department of Mechanical Engineering and Centre for Intelligent Machines, McGill University, Montreal*, 2010.

[5] H. C. Martin, *Introduction to matrix methods of structural analysis*. McGraw-Hill, 1966.

[6] A. Klimchik, D. Chablat, and A. Pashkevich, "Advancement of MSA-Technique for Stiffness Modeling of Serial and Parallel Robotic Manipulators," in *ROMANSY 22 – Robot Design, Dynamics and Control* (V. Arakelian and P. Wenger, eds.), (Cham), pp. 355–362, Springer International Publishing, 2019.

[7] A. Klimchik, A. Pashkevich, and D. Chablat, "Msa - technique for stiffness modeling of manipulators with complex and hybrid structures," in *12TH IFAC SYMPOSIUM ON ROBOT CONTROL - SYROCO 2018* , (Budapest, Hungary), June 2018.

[8] A. Pashkevich, D. Chablat, and P. Wenger, "Stiffness analysis of overconstrained parallel manipulators," *Mechanism and Machine Theory*, vol. 44, no. 5, pp. 966–982, 2009.

[9] A. Pashkevich, A. Klimchik, and D. Chablat, "Enhanced stiffness modeling of manipulators with passive joints," *Mechanism and machine theory*, vol. 46, no. 5, pp. 662–679, 2011.

[10] A. Klimchik, A. Ambiehl, S. Garnier, B. Furet, and A. Pashkevich, "Efficiency evaluation of robots in machining applications using industrial performance measure," *Robotics and Computer-Integrated Manufacturing*, vol. 48, pp. 12–29, 2017.

[11] C. Corradini, J.-C. Fauroux, S. Krut, *et al.*, "Evaluation of a 4-degree of freedom parallel manipulator stiffness," in *Proceedings of the 11th World Congress in Mechanisms and Machine Science, Tianjin (China)*, 2003.

[12] V. Skvortsova and D. Popov, "Design of the parallel spherical manipulator for wrist rehabilitation," in *2019 3rd School on Dynamics of Complex Networks and their Application in Intellectual Robotics (DCNAIR)*, pp. 166–168, IEEE, 2019.

[13] A. Klimchik, A. Pashkevich, and D. Chablat, "Fundamentals of manipulator stiffness modeling using matrix structural analysis," *Mechanism and Machine Theory*, vol. 133, pp. 365–394, 2019.

[14] D. Popov and A. Klimchik, "Optimal planar 3rrr robot assembly mode and actuation scheme for machining applications," *IFAC-PapersOnLine*, vol. 51, no. 11, pp. 734–739, 2018.